

AD-A250 075

FOR REPRODUCTION PURPOSES

2

SECURITY



red)

GE		READ INSTRUCTIONS BEFORE COMPLETING FORM
1. RE	2. GOVT ACCESSION NO.	3. RECIPIENT'S CATALOG NUMBER
ARO 27863.1-MS	N/A	N/A
4. TITLE (and Subtitle)		5. TYPE OF REPORT & PERIOD COVERED
Tribology of Langmuir-Blodgett Films		Interim Technical Report
		6. PERFORMING ORG. REPORT NUMBER
7. AUTHOR(s)		8. CONTRACT OR GRANT NUMBER(s)
C.L. Mirley		DAAL03-91-G-0139
9. PERFORMING ORGANIZATION NAME AND ADDRESS		10. PROGRAM ELEMENT, PROJECT, TASK AREA & WORK UNIT NUMBERS
University of Connecticut Storrs, CT 06269-3136		
11. CONTROLLING OFFICE NAME AND ADDRESS		12. REPORT DATE
U. S. Army Research Office Post Office Box 12211 Research Triangle Park, NC 27709		March 1992
14. MONITORING AGENCY NAME & ADDRESS (if different from Controlling Office)		13. NUMBER OF PAGES
		25
		15. SECURITY CLASS. (of this report)
		Unclassified
		15a. DECLASSIFICATION/DOWNGRADING SCHEDULE
16. DISTRIBUTION STATEMENT (of this Report)		
Approved for public release; distribution unlimited.		
17. DISTRIBUTION STATEMENT (of the abstract entered in Block 20, if different from Report)		
NA		
18. SUPPLEMENTARY NOTES		
The view, opinions, and/or findings contained in this report are those of the author(s) and should not be construed as an official Department of the Army position, policy, or decision, unless so designated by other documentation.		
19. KEY WORDS (Continue on reverse side if necessary and identify by block number)		
Tribology, Langmuir-Blodgett Films		
20. ABSTRACT (Continue on reverse side if necessary and identify by block number)		
This report reviews some of the current theories of lubrication, friction and wear, and how these effects are measured. Special emphasis is placed on polymeric systems and the use of Langmuir-Blodgett films as lubricants.		

TRIBOLOGY OF LANGMUIR-BLODGETT FILMS

Technical Report No. 1

C.L. Mirley, J.T. Koberstein

March 1992

U.S. Army Research Office

Contract Number: 27863-MS

University of Connecticut
Storrs, CT 06269-3136

Approved for Public Release:

Distribution Unlimited

Approved for Release	
DTIC	
DTIC	
Unrestricted	
Justification	
By	
Distribution/	
Availability Codes	
Dist	Avail and/or Special
A-1	

92-11636



92 4 28 173



TRIBOLOGY OF LANGMUIR-BLODGETT FILMS

by

**Christopher L. Mirley
Polymer Science Department
Institute of Material Science
University of Connecticut**

2/6/92

TABLE OF CONTENTS

	page
I. INTRODUCTION	1
II BACKGROUND	
A. FRICTION THEORY	2
B. WEAR THEORY	5
C. LUBRICATION	9
III. MEASUREMENT OF FRICTION AND WEAR	13
IV. TRIBOLOGICAL STUDIES ON LB FILMS	16
V. REFERENCES	25

I. INTRODUCTION

The word tribology is derived from the Greek word for rubbing, *tribos*¹, and refers to the science and technology of interacting surfaces in relative motion. The nature of these interactions is generally addressed under the subject of friction behavior while the consequences or responses of a material to these interactions are the subject of wear behavior.

The basic law of friction was first put forth by Amonton in 1699 who defined the friction coefficient, μ , as being equal to the ratio of the frictional force to the normal force. This has been proven to hold for many sliding solid-solid systems, but does little to enhance our understanding of friction behavior based on material properties. Bowden and Tabor² in the 1930's began systematic scientific investigations into the friction behavior of moving solids and subsequently developed their Adhesion-Shearing theory of friction. The theory was based on the fact that at a molecular level, most solid surfaces are punctuated by surface irregularities called asperities. When two surfaces come into contact under an applied load, the asperities from opposing surfaces form welded junctions. In order for the surfaces to move, the junctions must be sheared. The coefficient of friction was therefore a function of contact area and shear strength of the junctions. However, the model could not explain several important experimental observations concerning the behavior of μ .

A more successful approach to describing friction behavior, begun in the late 1940's by Macks and Shaw and continued by Suh and Sin³ in the 1970's, used a three-term model. The frictional force and hence the friction coefficient were modeled as the sum of three terms: adhesion between flat surfaces, deformation of asperities, and deformation of surface/subsurface layers by wear particles and asperities (ploughing). This model was able to explain the differences between static coefficient of friction, μ_s , and kinetic coefficient of friction, μ_k , and the variation of μ_k with load, sliding velocity, and temperature. The relative contributions from each of the components to friction was determined by Suh using metals. However, they claim that the three cited mechanisms for friction are found to occur in metals, polymers, and ceramics but to significantly different extents.

The subject of wear is closely related to friction and is important both from a theoretical and economic point of view. There are many different mechanisms by which wear occurs and usually more than one is operating at any given time during solid-solid motion. The basic parameter of interest in wear is the wear rate which is generally equal to the dimensions of the wear track divided by the sliding distance. Adhesion theory was initially used to explain and/or predict wear behavior but was later replaced by the Delamination theory of Suh.³ The delamination theory is especially successful at modeling sliding wear processes. The primary mechanisms for sliding wear were identified as deformation of subsurface material, initiation and propagation of cracks, formation of wear sheets on surface, and ultimately delamination. This behavior was found to be dominant in metals and highly linear, crystalline polymers.

To combat the effects of wear, surfaces are often lubricated with a fluid or solid. There are two regimes in fluid lubrication with the most important for real applications being boundary lubrication. Studies of boundary lubrication made by Hardy, Tabor, and Adamson¹ among

others concluded that an absorbed, almost monomolecular film on the surface of the moving materials significantly lowered the coefficient of friction and greatly reduced wear. This effect was more pronounced for metal-metal or polymer-metal contacts than for polymer-polymer contacts.

Despite the extensive work and developments made in understanding the macroscopic properties of lubrication, the microscopic behavior of the film molecules at the solid interface is not well understood i.e. the role of interactions between organic molecules and surfaces, conformation of organics on the surface, their transfer from one surface to another, their migration on solid surfaces and their interaction with other adsorbates. Langmuir-Blodgett (LB) films seem well suited to address some of the above mentioned questions due to the fact that with LB films one is able to control molecular orientation, packing, chemical structure, and film thickness. This paper will present some of the studies that have been undertaken in the area of tribology of LB films. Also in this paper, the development of theories on friction, wear, and lubrication of metals, ceramics, and polymers (excluding composites) as well as their methods of measurement will be discussed more fully.

II. BACKGROUND

A. FRICTION THEORY

The existence of friction between two bodies sliding against one another has been known since antiquity. The first attempt at a qualitative description of friction is credited to Leonardo da Vinci (1560), but the first scientific investigation of frictional behavior is often attributed to Amontons who reported his results to the Royal Academy of Science in 1699.¹ The dimensionless quantity known as the coefficient of friction, μ , is obtained from Amontons' Law:

$$\mu = F/L \quad (1)$$

where F is the friction or tangential force and L is the load or force normal to an unlubricated surface sliding across a second surface. This law states that μ is independent of the apparent area of contact between the two surfaces. Amontons also asserted that μ always has a value of $1/3$ which was later shown to be false especially for very clean surfaces. Coulomb (1785) and Euler (1748) also worked on tribological problems.³ The former advancing the Roughness theory of friction while the latter tried to explain the difference between static and kinetic coefficients of friction.

It wasn't until the 1930's that a more microscopic approach to the study of the friction mechanism was initiated by Bowden and Tabor.² They subsequently developed the Adhesion-Shearing theory which was the predominant theory of friction for many decades. The essence of the theory is that all surfaces prepared by conventional engineering techniques are rough (see Figure 1), so that on a microscopic scale the surfaces are composed of "peaks and valleys";

the peaks are called asperities. When two unlubricated surfaces are brought together, contact primarily occurs between opposing asperities and welded junctions are formed (due to metallic, ionic, Van der Waals or other forces). To satisfy the kinematic requirements for sliding, the welded junctions must be sheared and the frictional force therefore depends on the interfacial shear strength as well as the true area of contact which is a function of the applied normal load and contact pressure:

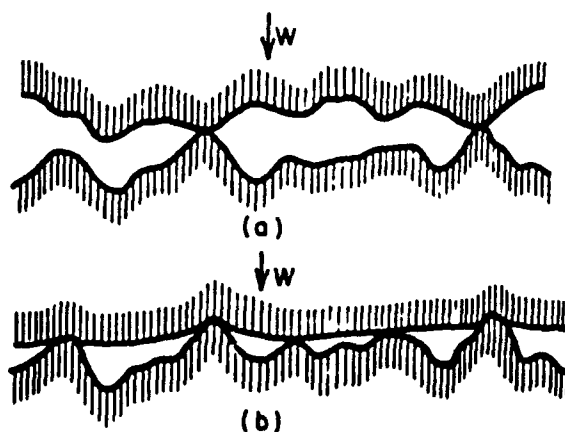
$$F = A_T \tau \quad (2)$$

$$A_T = L/P \quad (3)$$

$$\mu = \tau/P \quad (4)$$

where A_T is the real area of contact, τ is the interfacial shear strength or shear flow, and P is the contact pressure of the softer material which is related to the material hardness. Experimental results showed that the theoretical coefficients of frictions were generally much smaller than those determined experimentally and the differences were worse when the experiments were done in vacuum or an inert atmosphere.³ To explain these discrepancies, Bowden and Tabor argued that the true area must be larger under tensile loading, due to deformation of the junctions, requiring a larger force to shear the interface. Rabinowicz³ postulated that the increase in the actual area of contact is due to a contribution from the surface energy of adhesion when the materials are deformed plastically. By using the definition of work of adhesion and the surface energies of the materials, he showed

Figure 1: Comparison of Actual Contact Areas for
a) Metal-on-Metal and b) Polymer-on-Metal. Adamson.¹



mathematically that an extra term in A_T arises from considering the interfacial energy change. However, the small changes in surface energy compared to the total work done were found to be quite small and usually negligible.

Tabor⁴ then proposed a two-term model to describe the friction behavior of unlubricated solids which addressed the following issues: 1) The area of true contact between sliding surfaces; 2) The strength of the bond that is formed at contact points; 3) The way in which the material in and around the contacts is deformed. According to this model, the total frictional force is the sum of friction due to adhesion and to deformation or ploughing. This is essentially the Adhesion-Shearing model but with an extra term. The deformation or ploughing term becomes prominent for hard surfaces sliding against a softer surface. In this case, the hard asperities dig or plough into the softer surface causing very large shear strains at the surface even if the interfacial adhesion is quite small. It is these large shear strains at the surface layers which leads to formation of thin flakes; a process called delamination.

This new model, however, still could not account for some of the observed friction behavior between solids such as the effect of entrapped wear particles, the time dependency of μ , and the changes in μ when material roles are reversed during friction testing. Another approach to friction behavior developed by Shaw and Macks (1949), Kragelskii (1980), and Suh and Sin (1981)³ uses a three-term friction model. Here, the total frictional force is the sum of friction due to asperity deformation, ploughing both by hard surface asperities and wear particles, and adhesion between flat surfaces. The coefficient of friction can then be written as:

$$\mu = \mu_{\text{def}} + \mu_{\text{plo}} + \mu_{\text{adh}} \quad (5)$$

The relative roles and contributions of each of these terms to the total frictional force have been defined by Suh and are given as follows: 1) Asperity Deformation. The asperity deformation term mainly determines the magnitude of the static friction coefficient, μ_s . It also contributes to the kinetic friction coefficient, μ_k , but is not large relative to the contributions from ploughing and adhesion due to the fact that once the asperities are sheared off, new asperities can only be formed through delamination of wear particles. This occurs only after a large number of load cycles; 2) Adhesion Component. This frictional force is a function of the adhesion between two opposing surfaces. The adhesion force is due to the welding of two nearly flat portions on the opposing surfaces or to interatomic interaction between atoms that are brought into close proximity. Adhesion can also arise at the slopes of two interacting asperities, but this frictional contribution is already taken care of in the deformation term. At the onset of sliding, μ_{adh} is not present or is at least negligible which may be due to the presence of contaminants on the surface. When deformation of asperities occurs, new surfaces are created which can then adhere to each other and the adhesion frictional force increases. 3) Ploughing Component. The frictional force from this term can be due to either hard asperities or penetration of wear particles. When the surfaces are both hard, the wear particles can penetrate the surfaces equally and grooves can be formed in one or both of the surfaces. When one of the surfaces is harder than the other, the wear particle will simply slide along the hard surface so that no ploughing can occur. However, if the hard surface is very

rough, the wear particles tend to become anchored in the hard surface and plough the softer surface.³ The contribution of ploughing to the friction coefficient is sensitive to the ratio of the radius of curvature of the particle to the depth of penetration.

Using slip-line field analysis, exact equations for μ_{def} , μ_{plo} , and μ_{adh} were developed by Suh. Generally, these are as follows:

$$\mu_{\text{def}} = \phi \quad \mu_{\text{adh}} = \tau/k \quad \mu_{\text{plo}} = w/2r \quad (6)$$

where ϕ = average slope of the asperities.
 τ = shear stress at the interface.
 k = shear flow strength of the softer material.
 w = width of wear particle penetration.
 r = radius of wear particle.

Based on experiments using an iron-carbon system, the relative contributions of each of the friction terms was evaluated: for the deformation of asperities, $\mu_{\text{def}} \sim 0.43 - 0.75$; for the adhesion component, $\mu_{\text{adh}} \sim 0 - 0.4$; for the ploughing term, $\mu_{\text{plo}} \sim 0 - 1.0$. It is apparent from this analysis that the ploughing contribution to the total overall friction can be quite large.

In addition to the above three friction components, there can be other contributions to friction such as viscoelastic surfaces of polymers which show large hysteresis losses, and wear particles that are also viscoelastic which become stuck at the interface consume energy through repeated deformation.

In conclusion, Suh has pointed out that the friction generating mechanisms of deformation, adhesion, and ploughing should occur in case of ceramics, most thermoset plastics and thermoplastics, as well as most metals. In addition, some materials like PTFE and polyethylene are also affected by molecular orientation at their interfaces. Above all it should be noted that friction behavior is affected by the kinematics of the surfaces in contact, the externally applied forces, environmental conditions, surface topography, and materials properties. Therefore the coefficient of friction is not simply a material property parameter.

B. WEAR THEORY

The wear of materials can occur by many different mechanisms which depend on the properties of the materials, the operating conditions, and the geometry of the wearing bodies. The treatment of wear behavior can therefore be of considerable complexity and it is only within the past three decades that the essential scientific foundations for its description have been laid down. The classification of these wear regimes can be divided into two groups: those due primarily to the mechanical behavior of the solid and those due to the chemical behavior of materials.^{3,5,6} Table 1 lists the wear processes under each of these regimes as well as the characteristics and situations where they are commonly encountered. In a majority of wear situations, there is more than one mechanism operating at the same time, but usually one can be identified as the rate-determining mechanism. According to Suh³, the factors that

determine the dominant wear behavior are the mechanical properties/chemical stability of materials, temperature, and operating conditions. Whatever the cause, it is now clear that the economic cost of wear on a national scale is enormous i.e. the reported cost of tire replacement in U.S. naval aircraft alone is on the order of $\$2 \times 10^6$ per year.⁶

1) Mechanical Wear Processes. Included in this regime are sliding or adhesive wear, abrasive wear, and fatigue wear. Sliding wear occurs most often between surfaces where one of the surfaces is very clean, smooth, and rigid. These lead to high shear strength adhesive junctions between the surfaces, which in response to an applied shear stress, leads to film transfer of the softer surface layer to the counter surface. Repeated moderate-speed sliding motion leads to delamination of the transferred film and the entire process is repeated. Well known examples of this type of wear are PTFE and HDPE. The reason for the transfer of thin films in the case of

Table 1: Classification of Wear Processes. Suh.³

(a) Wear processes that are dominated primarily by the mechanical behavior of materials under a given loading condition

Type	Typical Characteristics and Definitions	Observed In:
Sliding wear (delamination wear)	Plastic deformation, crack nucleation, and propagation in the subsurface.	Sliders, bearings, gears, and cams, where surfaces undergo relative motion.
Fretting wear	The early stages of fretting wear are the same as sliding wear but depend on relative amplitude. The entrapped wear particles can have significant effect on wear. The relative displacement amplitude is important.	Press fit parts with a small relative sliding motion.
Abrasive wear	Hard particles or hard surface asperities plowing and cutting the surface in relative motion.	Sliding surfaces, earth-removing equipment.
Erosive wear (solid particle impingement)	Due to solid particle impingement, large subsurface deformation, crack nucleation, and propagation. Sometimes, the surface is cut by solid particles when the impingement angle is shallow.	Turbines, pipes for coal slurries, and helicopter blades.
Fatigue wear	Fatigue crack propagation takes place, normally perpendicular to the surface, without gross plastic deformation under cyclic loading conditions.	Ball bearings, roller bearings, and glassy solid sliders.

(b) Wear processes that are controlled primarily by chemical processes and thermally activated processes

Type	Typical Characteristics and Definitions	Observed In:
Solution wear	Formation of new compounds of a lower free energy of formations; high temperature; no gross plastic deformation; atomic-level wear process.	Carbide tools in cutting steel at high speeds.
Diffusive wear	Diffusion of elements across the interface.	High-speed-steel (HSS) tool in cutting steel at high speeds.
Oxidative wear	Formation of weak, mechanically incompatible oxide layer.	Sliding surfaces in highly oxidative environment (not common).
Corrosive wear	Corrosive of grain boundaries and formation of pits.	Lubricated and corrosive atmosphere.

these two polymers is thought to be due to their highly crystalline morphology and smooth molecular profiles (this is also the explanation for their low coefficients of friction). Other polymers such as LDPE which tend to have rough molecular profiles show "lumpy transfer".⁵ The simplest physical picture of abrasive wear is one in which hard surface asperities or hard wear particles penetrate the opposing surface and remove material by ploughing or microcutting. These processes are respectively called two-body and three-body abrasion. Fatigue wear is routinely found in materials that have low moduli when sliding against very rough surfaces. This type of wear leads to tearing, crack formation and propagation, and ultimately bulk failure.

2) Chemical Wear Processes. Chemical degradation most certainly occurs in all forms of wear.⁵ They are predominant however under conditions where sliding speeds between surfaces are high (diffusive and solution wear) or at high temperatures in highly oxidative environments (corrosive and oxidative wear). The effects may range from surface delamination to gross decomposition.

There are several parameters used to quantify wear processes.⁶ The basic parameters of interest are shown below:

$$W_h = h/d \quad (7)$$

$$W_v = V/dL \quad (8)$$

where W_h = depth wear rate.
 W_v = volumetric wear rate or abrasion factor.
 h = thickness removed.
 d = sliding distance.
 V = wear volume.
 L = normal load.

When the most serious consequence of wear is the loss in fit of a component, it is common to use the parameter W_h . The volumetric wear rate is a more fundamental parameter which arises from several theories of wear.³ There are also a variety of units used for the various wear parameters. The terms *wear resistance* and *abrasion resistance* are also widely used and correspond to the reciprocal of the wear rate.

For two materials sliding against one another, the wear volume is almost linearly proportional to the distance slid and normal load, but inversely proportional to the hardness of the worn material. This can be expressed mathematically as follows:

$$V = K (Ld/3H) \quad (9)$$

where H is the hardness and K is a dimensionless proportionality constant known as the wear coefficient. It should be noted that the ratio L/H is equal to the real area of contact A_r . Abrasive wear in metals follows the relationship given by Eq (9) quite well with typical values of the

wear coefficient of 10^{-2} to 10^{-1} .

All of the wear phenomenon listed in Table 1 were initially explained in terms of the adhesion theory until the development of delamination theory for sliding wear by Suh (1973).³ The adhesion theory for wear was identical to that for friction i.e. the wear of materials is due to the welding of asperity junctions, which create a hemispherical wear particle when the weaker material fractures near the weld junction. The problems found with the theory were that it violated the conservation of energy law and it could not be used to form the basis for developing wear resistant materials.

Shaw³ showed that the wear coefficient could be rewritten as follows:

$$\begin{aligned} K &= 3VH/Ld \\ &= V/A_T d \\ &\sim V/A_P d \end{aligned} \quad (10)$$

where A_P is the cross-sectional area of the plastically deformed zone under the asperity contact. The physical significance of the wear coefficient is now clear; K represents the ratio of the worn volume to the volume of the deformed zone. Usually K is on the order of 10^{-4} to 10^{-3} and this indicates that the volume of material removed by wear is a very small fraction of the material undergoing plastic deformation. Therefore the primary mode of energy dissipation in sliding wear is through deformation of the subsurface beneath asperities and it is impossible to model this behavior without taking into account this deformation process.

The delamination theory of wear describes the following chain of events leading to wear sheet formation during sliding wear: 1) Sliding surfaces contact through the asperity points. Asperities of the softer material are deformed and fractured forming small wear particles. Hard asperities are also formed but at a slower rate. 2) Surface stresses exerted by the harder asperities at the contact points induces incremental subsurface plastic deformation per cycle of loading. 3) As the subsurface deformation continues, cracks are nucleated. Once cracks are present, further loading causes the cracks to propagate parallel to the surface at a depth governed by the properties of the material and loading conditions. 4) When the cracks finally shear to the surface, long and thin wear sheets delaminate. The wear is controlled by the crack nucleation rate or crack propagation rate whichever is slower.³ Suh has substantiated this theory by a series of experimental studies with iron and steel but the same type of behavior is found to occur in polymers as well, although polymer-polymer combinations tend to have the highest wear rates due to poor heat conductivity. For glassy or amorphous polymers, the failure of the subsurface occurs when the maximum tensile strength exceeds the cohesive strength of the polymer. Cracks are nucleated and propagate right at the asperity contact producing lumpy wear particles. For highly symmetric and crystalline polymers without bulky side groups, the molecules at the surface elongate and align themselves parallel to the direction of the shear force. These highly stretched molecules, which are held together by weak secondary forces, are then sheared off from the solid surface. Glassy polymers tend to exhibit high coefficients of friction and chunky wear particles, while highly linear polymers have low

coefficients of friction and wear debris consisting of thin film sheets.

Abrasive wear was modeled as a cutting process. Rabinowicz's theory, which is a commonly cited work³, states that the volume of material cut is equal to the volume displaced by the wear particle. Because of this, it was shown that the wear coefficient was related to the geometry of the asperity as follows:

$$K = (3 \tan \theta) / \pi \quad (11)$$

where θ is the average slope of the asperities. The same model for the friction coefficient due to ploughing gives $\mu = \tan \theta / \pi$, so that:

$$K = 3\mu \quad (12)$$

The wear coefficient is therefore directly related to the friction coefficient.

C. LUBRICATION

In order to reduce the damage caused by wear processes to sliding surfaces, a gas, liquid, or solid can be placed in between the contacting surfaces which acts as a lubricant to lower the friction coefficient and hence resistance to motion. Generally, there are two lubrication regimes^{1,6}: 1) Hydrodynamic or elastohydrodynamic. In this regime, the fluid film is thick enough so that the solid surfaces are essentially independent of each other and the coefficient of friction depends only on the shear properties (i.e. viscosity) of the fluid. 2) Boundary Lubrication. Under heavy loads and low-to-moderate sliding speeds, the fluid film thins out and increasing contact occurs between the surface regions. The coefficient of friction rises from the low value for fluid friction to some value which is less than that for the unlubricated surface. Figure 2 shows a plot known as a Stribeck curve which illustrates this behavior. The abscissa values on the plot are (viscosity x speed)/(load) which is called the generalized Sommerfeld number.

Much of the work on boundary lubrication was carried out by Sir William Hardy using hydrocarbon-type lubricants like long-chain paraffins, alcohols, and acids on metals. He concluded that the lubricants adsorbed to the surface of the metals and lead to a "reduction in the fields of force between the surfaces".¹ Hardy's work, which was extended by Zisman, Frewing, and Tabor², indicated that the main function of the boundary film was to reduce or if possible eliminate contact between surfaces. In addition, if the friction coefficient was to be low, the film must be easily sheared. It is for this reason that long-chain organic molecules were found to be particularly well suited as boundary lubricants. The films themselves are very thin or even monomolecular and in general the greatest protection to the surfaces is provided when the boundary film is in the condensed state. Therefore, paraffins, long-chain alcohols, and amines were found to be effective for reducing friction at temperatures up to their melting points. Fatty acids were effective to temperatures beyond their melting point due to formation of fatty acid soaps through interaction with the metal or metal oxide surfaces. Unsurprisingly,

the coefficient of friction was found to decrease and level off to a minimum with increasing molecular weight of these lubricants. Tabor also correlated this effect to the increase and leveling off of the contact angle. Figure 3 is a diagram depicting the phenomenon of boundary lubrication.

Hardy's initial explanation of the causes of boundary lubrication were in a general correct

Figure 2: Stribeck Curve. Regimes of Boundary and Hydrodynamic Lubrication. Adamson.¹

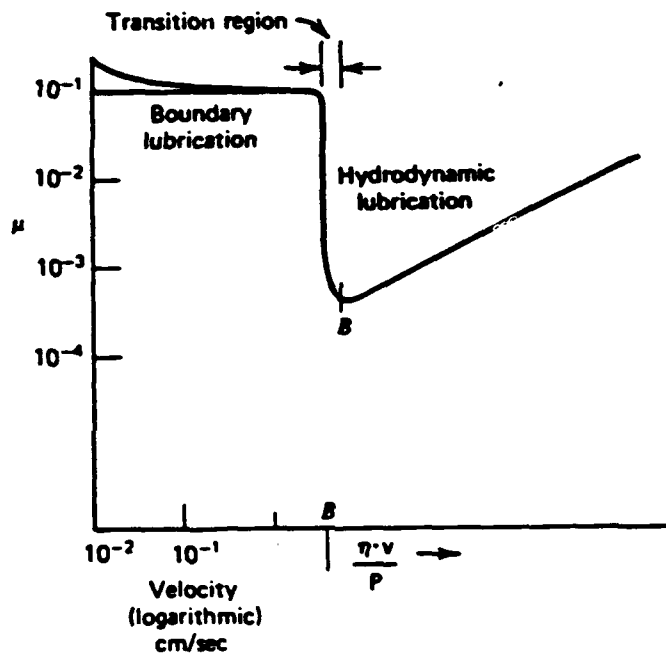
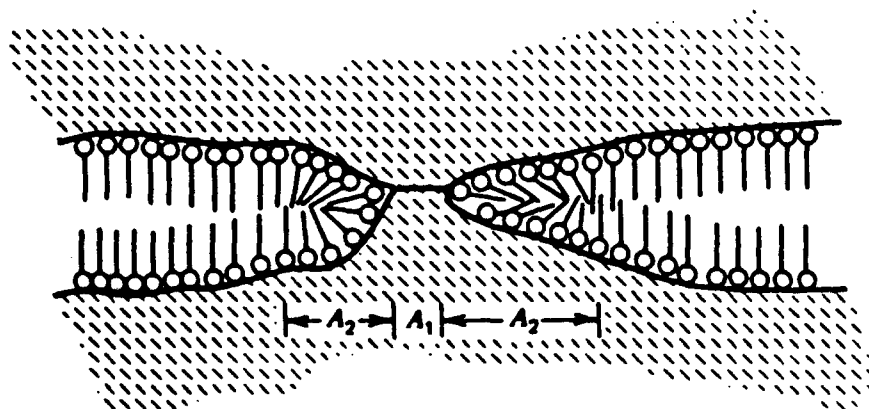


Figure 3: Nature of the Contact Region in Boundary Lubrication. Adamson.¹



but could not explain several important observations. First, it was found that with very light loads, the coefficient of friction increased to values approaching that for the unlubricated surface. Secondly, even under normal boundary lubrication conditions where μ is small, surface-surface contacts were still present. Radioautographic studies by Bowden and Tabor² showed that boundary lubrication reduced the magnitude of the contacts not the number of contacts. Therefore various boundary lubricants can give about the same coefficient of friction yet differ enormously in the amount of wear allowed.

To account for these observations, Adamson developed a pressurized-film model for boundary lubrication. The mechanism of boundary lubrication is pictured as follows: under boundary lubrication, there are regions of surface-surface contacts due to prominent asperities surrounded by regions of fluid-fluid contact. At small loads the surrounding fluid film fringe is essentially that of a normal monolayer. The load is then being supported both by the asperity contacts and film-film contacts (Figure 3). The total frictional force can be written as:

$$F = A_1 s_m + A_2 s_f \quad (13)$$

where A_1 = surface-surface contact area.

A_2 = fluid-fluid contact area.

s_m = shear strength of surface-surface contacts.

s_f = shear strength of fluid.

It is clear that at small loads the fluid term in Eq (13) makes more of a contribution to the friction force than the term due to solid contacts. Therefore, Amonton's law should not be obeyed and the coefficient of friction should be at values close to those for the unlubricated surface to the extent that it arises from A_1 . Also, in the case of hydrocarbon lubricants s_f may be fairly large due chain entanglement.

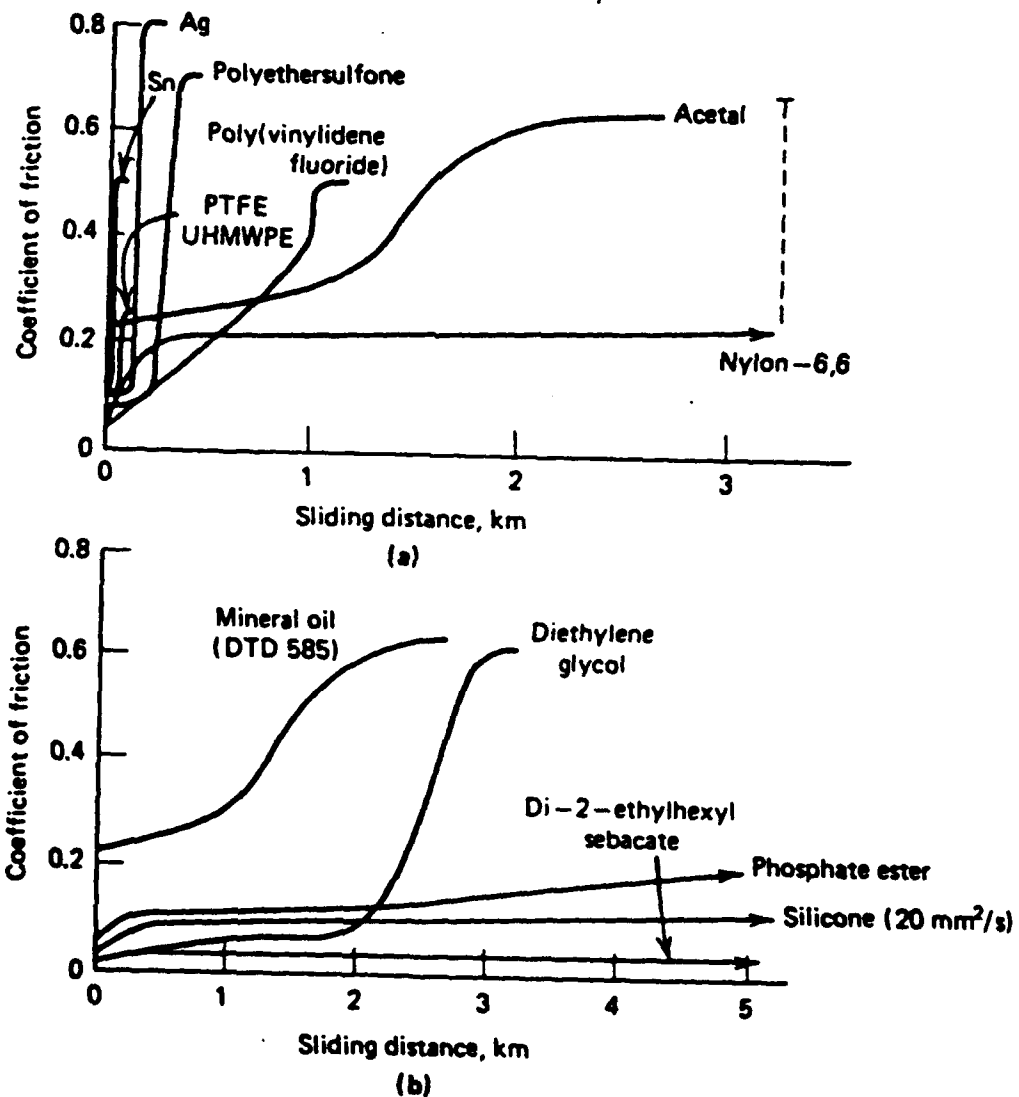
Moderate to large loads will tend to increase the area of solid-solid contacts, however much smaller loads are sufficient to place relatively large areas of the fluid film under varying mechanical pressure so that most of the load is floating on pressurized film.¹ To the approximation of Eq (13), A_2 the area of the film is proportional to the applied load and Amonton's law should be obeyed. Additionally, the shear strength of the fluid, s_f^* , now applies to film molecules which are lying flat and is taken to be much smaller than s_f or s_m . Therefore one should observe low μ values under boundary lubrication conditions with normal loads.

Reduction in friction by adsorbed hydrocarbon boundary lubricants is relatively small in the case of polymer-polymer contacting surfaces. This is due to the inability to form close-packed monolayers on polymers⁷ and because the shear strength of hydrocarbon lubricants is not very different from those of polymers themselves. However, boundary lubrication is effective for metal-metal and polymer-metal contacts. In these cases reduction in friction is significant because of the ability of the lubricants to adsorb to the metal surfaces.¹

Figure 4 shows plots of μ versus sliding distance for several polymers and metals in contact

with stainless steel as well as the effects of various lubricants. There are marked differences in the magnitude and behavior of the friction coefficient as the materials and lubricants are varied.

Figure 4: Effect of Materials and Lubricant on μ . a) Various Polymers and Metals with Mineral Oil. UHMWPE is Ultra High Molecular Weight Polyethylene. b) Acetal Resin with Various Fluids. Counter Surface- Smooth Stainless Steel ($0.15 \mu\text{m } R_a$) with $0.5 \mu\text{l}$ of Fluid Added Following Initial Dry Sliding. Lancaster.⁶



III. MEASUREMENT OF FRICTION AND WEAR

There are a variety of devices for assessing friction and wear of materials. The equipment ranges from the very simple i.e. those designed to specifically study the basic mechanisms by which surface damage is initiated and propagated to the more complex i.e. those that are custom-built to simulate the operating conditions of a particular application. Intermediate between these two cases is equipment which is capable of ranking materials in different wear regimes under various experimental conditions like load, speed, or temperature.⁶ Regardless of which device is chosen, the components for measuring friction are essentially the same; a stationary member (the slider) is rubbed against a moving member (the specimen). The load or normal force (L) is applied using dead weights and the tangential or frictional force (F) is measured using a strain gauge. The kinetic coefficient of friction is then obtained from the ratio F/L . Wear rate can be measured by determining the weight changes of the specimen and slider, by measuring the topological profile of the worn surface, or by measuring dimensional changes in the slider.³

Figure 5 shows a schematic diagram of the more widely-used equipment which fall into the intermediate device category stated above. Apparatus of the pin-on-ring or pin-on-disk type (5a and b) is particularly suitable for wear measurements of polymers sliding against metals. If the metal surface is smooth, and the location of a polymer pin remains fixed, wear is of the delamination type as in a bearing. Deformation wear is induced by roughening the metal surface or covering it with an abrasive material. Figures 5c and 5d simulate journal and thrust bearing applications respectively. The difference in these configurations is that it is much harder for the wear particles to escape from the contact zone. This modifies the wear mechanism and hence the structure and thickness of the transfer films generated on the counter surface. Three-body abrasion is simulated by introducing loose particles or particles dispersed in a fluid to the contact areas.

Devices 5e and 5f are used extensively for fundamental studies at relatively high stresses the conical element in 5e and the top ball in 5f are usually steel. However, device 5f has been used in reverse with three steel balls and one polymer ball or the polymer ball replaced by a cone.⁶ The remaining devices, 5g-j, are primarily intended for abrasion/erosion studies on elastomers. In 5g, flat samples are worn against abrasive paper or cloth, while in 5h one or more rubber wheels driven against a rotating disk simulate certain aspect of tire wear. Three-body abrasion is simulated in device 5i where the polymer pad can be either stationary or rotating. Lastly, device 5j is able to assess erosive wear of a wide range of materials, either as shown or with the specimen itself rotating in a stationary container of abrasive particles. Many of these devices have been incorporated into ASTM standard test procedures. Table 2 lists friction coefficient and wear rate data for various polymers using some of the equipment described above.

A device developed by Tabor, Winterton, and Israelachvili¹ called the Surface Force Apparatus (SFA) for measuring the forces between two mica surfaces as a function of separation, has recently been modified to measure the friction coefficient of any material capable of being coated onto the mica surfaces. A modified SFA used by Briscoe to measure the

Figure 5: Schematic Arrangements of Various Types of Wear-Testing Apparatus:
a) Pin-on-Ring b) Pin-on-Disk c) Block-on-ring d) Thrust Washers e) Cone and Washer
f) Four Ball g) Tape Abrader h) Rolling with Slip i) Pin and Disk-Loose Abrasion
j) Abrasive Erosion. Lancaster.⁶

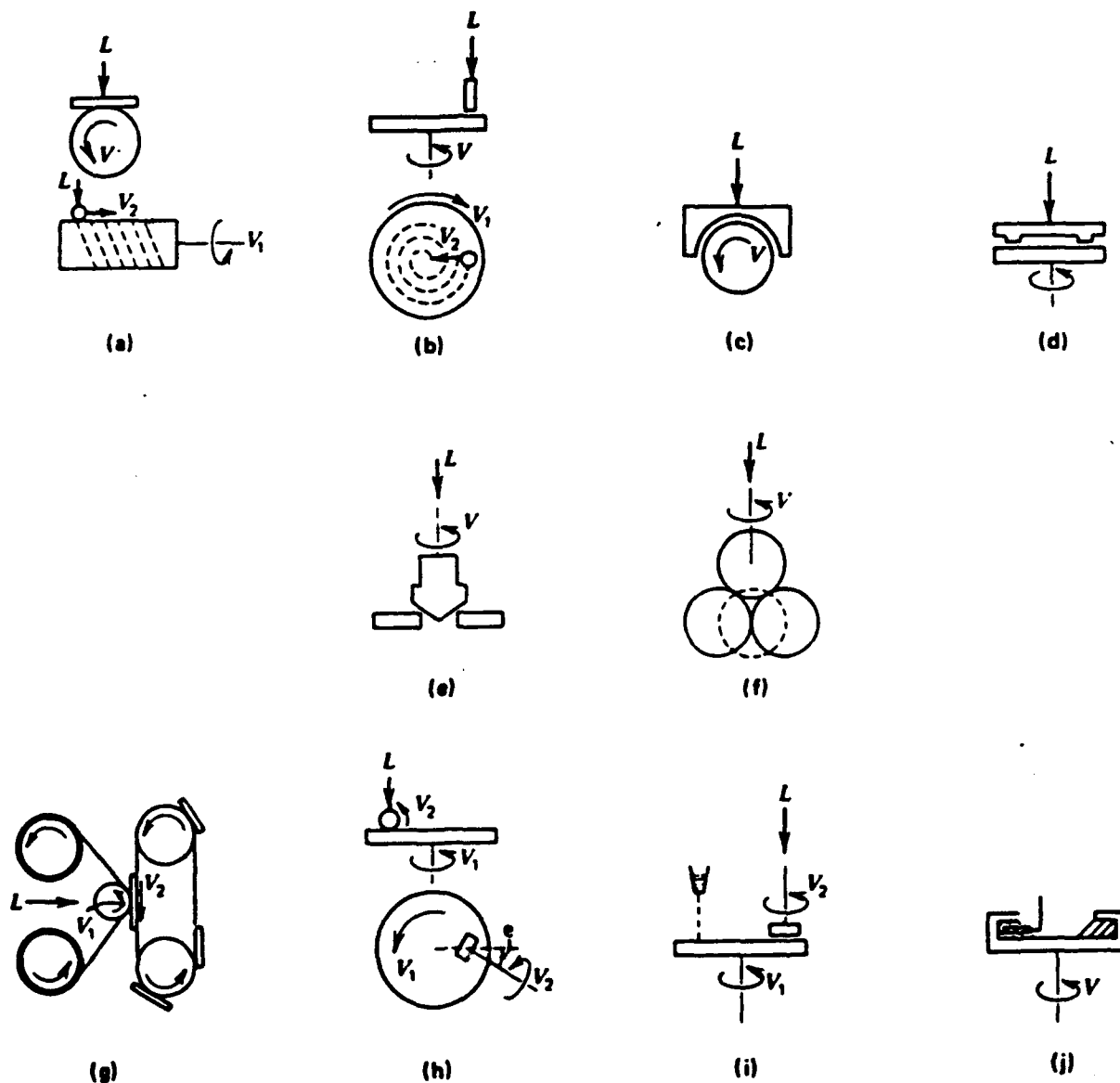


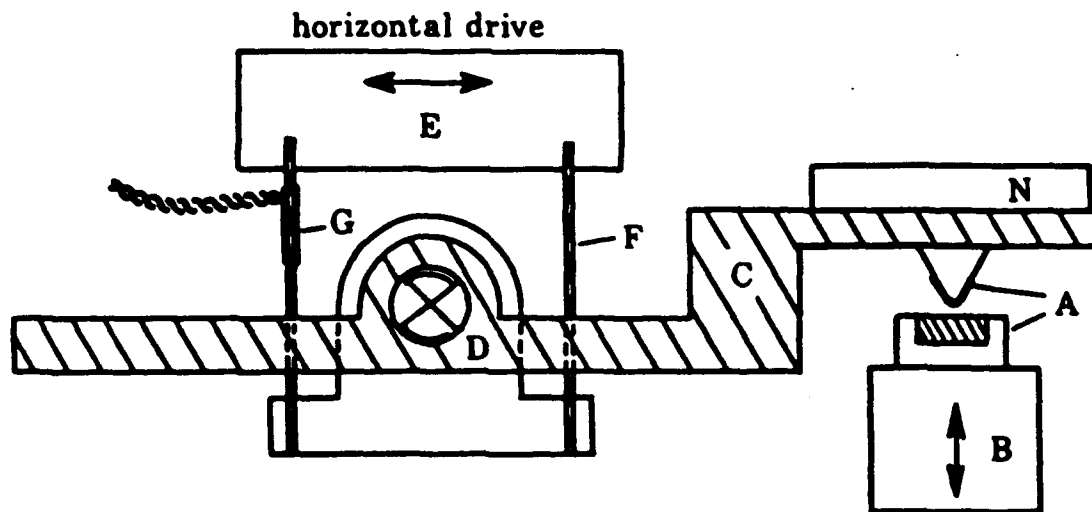
Table 2: Friction and Wear Data of Polymers. Suh.³

Material	Normal Load (g)	Sliding Speed (cm/sec)	Coefficient of Friction	Wear Rate (g/cm)
HDPE	200	3.3	0.31	1.1×10^{-9}
	450	3.3	0.25	2.7×10^{-9}
		16.4	0.25	5.5×10^{-10}
		33.	0.25	6×10^{-10}
POM ^b (Delrin)	200	3.3	0.22	1×10^{-8}
	450	3.3	0.31	1×10^{-8}
PMMA	200	3.3	0.64	4×10^{-8}
	450	3.3	0.68	8×10^{-8}
PC (Lexan 101)	450	3.3	0.6	2.5×10^{-8}
PC (Lexan 121)			0.5	2.4×10^{-8}

* Experimental conditions: geometry, pin on disk (AISI 52100 steel pin); test done at room temperature (22°C); atmosphere, air; relative humidity, 65%.

^b Sometimes known as acetal.

Figure 6: Surface Force Apparatus. A-Mica Surfaces, B- Lower Support with Vertical Adjustment, C- Lever Area, D- Flexure Pivot, E- Horizontal Drive for the Friction Area, F- Cantilever Springs, G- Resistance Strain Gauge Elements, N- Dead Load. Briscoe.⁸



friction behavior of LB films is shown in Figure 6. Essentially, two glass prisms are covered by molecularly smooth, conforming mica sheets and mounted orthogonally into the SFA. When a weight N is applied, a small elliptical contact area is formed at the surfaces. The interfacial contact area is measured very accurately by using multiple beam interferometry. If the backs of the mica sheets are silvered, then collimated white light directed onto one of the surfaces is transmitted and focused to give an image of the contact area. Stiff cantilever springs which support the upper prism are mounted with strain gauges that monitor the frictional forces when the lower prism is displaced laterally. A similar arrangement has also been used by Homola et. al. to measure the interfacial sliding friction of molecularly smooth surfaces.⁹ The advantages of these devices is that 1) The true molecular area of contact, the deformation, and lateral motion of the surfaces can be monitored simultaneously by recording the interference images of the mica surfaces. 2) The frictional behavior of any material capable of being coated on the mica sheets can be measured.

Another type of force sensing instrument, one which may lead to an understanding of the dynamics of friction on the atomic scale, is the atomic force microscope (AFM). The AFM technique involves the use of a sharp tip (one molecule at its point) to measure the friction force as the tip is rastered across a surface. The force on the tip is measured by detecting the deflection of a spring element on which the tip is mounted by either electron tunneling or optical interferometry. With its high spatial resolution, the AFM can provide information about surface forces complementary to that provided by the SFA. Erlandsson et. al. have used the AFM technique to study the friction between mica and a tungsten tip.¹⁰ They were able to detect frictional forces which varied with the periodicity of the hexagonal layer of SiO_4 units that formed the cleavage plane of the mica sample.

Other instrumentation which has been used to study the friction and wear behavior of materials includes surface analytical tools such as X-ray Photoelectron Spectroscopy (XPS) and Auger spectral analysis, and grazing incidence FTIR (GIIR).⁵

IV. TRIBOLOGICAL STUDIES ON LB FILMS

The effects of insoluble monolayers at air/water interfaces have been known at least since the time of Aristotle¹¹ and have been scientifically studied by such notable individuals as Benjamin Franklin, Lord Rayleigh, and Langmuir and Blodgett for whom the process of preparing thin solid films from water surfaces is named (even Margaret Thatcher has made contributions to this field). Not all substances are capable of forming insoluble monolayers at gas/liquid interfaces. Those that are however can be classified simply into two groups: polymeric and nonpolymeric.¹² Nonpolymeric substances are the "classical" monolayer materials and their ability to form monolayers is due to their amphiphilic properties; one portion of the molecule is attracted to the liquid or subphase while the other usually larger portion is repelled by it. The delicate balance between these forces determines whether or not a molecule will form an insoluble monolayer. Examples of these materials used to form

monolayers on water include fatty acids (greater than C_{10}), alcohols, amines, polycyclic aromatic hydrocarbons, heterocyclic compounds, and various combinations of these.^{11,12} In the case of polymeric materials, somewhat different criteria apply for monolayer formation. Unlike the "classic" monolayers, a high degree of insolubility is not required. It is only necessary that the monomer units of the polymer have a finite free energy of adsorption from the bulk spreading solution to the subphase surface. In other words, the polymers must have sufficient attraction for the surface to overcome bulk cohesion.¹² It is therefore possible to prepare LB films from polymers which are water soluble. Some examples of these materials investigated include poly(acrylates), PMMA, PVA, poly(vinyl fluoride), poly(siloxanes), liquid crystal polymers, and some polypeptides. Polymeric monolayers can be prepared as preformed films or prepared *in situ* after being deposited as monolayers. Examples of the latter are poly(vinyl stearate), a poly(styrene) derivative, and diacetylenes.¹¹

The commercial interest in using LB films is well documented^{11, 12, 13, 14} and designated applications for these thin films include optical wave guides, biosensors, electronic transducers, filters, insulating layers, and photoresists to name a few. LB films have also been of great interest as model systems in many areas of research. One important area where LB films could make a scientific and commercial impact is in the field of lubrication. Fundamental studies on the microscopic behavior of lubricants using LB films could help address such questions as the role of interactions between organic molecules and surfaces, conformation of organic molecules at surfaces, and their migration on solids. An important area of application for LB films as lubricants is in magnetic recording.^{15,16} The challenge here is finding coatings for the magnetic media which will be good permeability barriers for the metal oxide surface of tapes, good lubricants which avoid wear of the tape during use, and are as thin as possible.

An earlier study carried out by Rabinowicz and Tabor² on the friction behavior of fatty acid boundary lubricants was recently extended by Briscoe and Evans.⁸ It was noted by Tabor that a single hydrocarbon monolayer strongly adsorbed on to the surfaces of two sliding solid substrates could provide effective lubrication. For two such monolayers to remain intact, all the shear during sliding must occur by the motion of one layer of hydrocarbon chains over another.

In their study, Briscoe and Evans used a surface force apparatus (SFA), which is shown in Figure 6, to study the mechanisms controlling the friction in monolayer lubricants composed of C_{14} to C_{22} fatty acids, calcium soaps, and partially fluorinated fatty acids. The mica sheets of the SFA were coated with single monolayers using a Langmuir trough. Since the mica is a hydrophilic material, the polar head groups of the fatty acids should be attached to the surface with the hydrocarbon chains sticking up. The soaps are very similarly arranged however it is expected that metal ions should also be incorporated between the monolayer and surface.¹² Molecular areas of 0.21 nm^2 were found for most of the materials which was close to their X-ray cross section in the bulk crystal. This ensured that the monolayers were densely packed

though not necessarily in the crystalline state.

The frictional parameter measured was the interfacial shear strength τ which was obtained in all experiments by dividing the sliding force by the area of contact (see Eq (2) and (4). Note that τ is proportional to the friction coefficient). The advantages of using SFA in these experiments was that the area of contact during sliding and the monolayer film thicknesses (wear) could be very accurately measured by multiple beam interferometry. It was observed that while most of the fatty acids showed continuous motion, certain soaps showed discontinuous or 'stick-slip' motion. However no changes in contact area or film thickness were found in either cases.

The shear strength was measured as a function of contact pressure P , sliding velocity V , and temperature T . The variation of shear strength with each of these variables was shown to be governed by linear relationships of the following type:

$$\tau = \tau_0 + \sqrt{P} \quad \text{at constant } V, T \quad (14)$$

$$\tau = \tau_0^* - \beta T \quad \text{at constant } P, V \quad (15)$$

$$\tau = \tau_0^{**} + \theta V \quad \text{at constant } P, T \quad (16)$$

where $\tau_0, \tau_0^*, \tau_0^{**}, \sqrt{P}, \beta, \theta$ are constants. Table 3 lists some of these constants determined for the monolayers from the experimental data. These equations are similar to those found for bulk materials. In all cases, the shear strength increased with pressure and decreased with temperature. However, shear strength increased with velocity for the acids but decreased for the corresponding soaps. Also the results were found to be relatively insensitive to the chain length but significant differences in the magnitude of τ and the equation constants between the fatty acids and there corresponding saponified and fluorinated analog were observed

A rather interesting result found was that for the fluorinated monolayers. Figure 7 shows shear strength versus contact pressure for both stearic acid and fluorinated stearic acid. The absolute values for τ of the fluorinated acid were two to four times those found for the acid. Since PTFE is known to have the lowest friction coefficient of any polymer ($\mu = 0.09$), the results for the fluorinated monolayer were surprising. Tabor has noted however that not all polymers which expose fluorine atoms are low friction materials; for example a fluorinated epoxy developed to be water resistant showed very good adhesion and had a high friction coefficient.⁴ This strongly suggests that chemical structure and morphology both have significant influences on the friction behavior of materials.

Figure 8 shows τ versus P for monolayers of stearic acid having different degrees of saponification. It is known that the higher the pH of the water subphase, the higher the degree of salt formation. As shown in Figure 8, the stearic acid monolayer with the highest salt formation shows a lower shear strength than the acid. The intermediate concentrations of calcium stearate are the same or higher than the stearic acid.

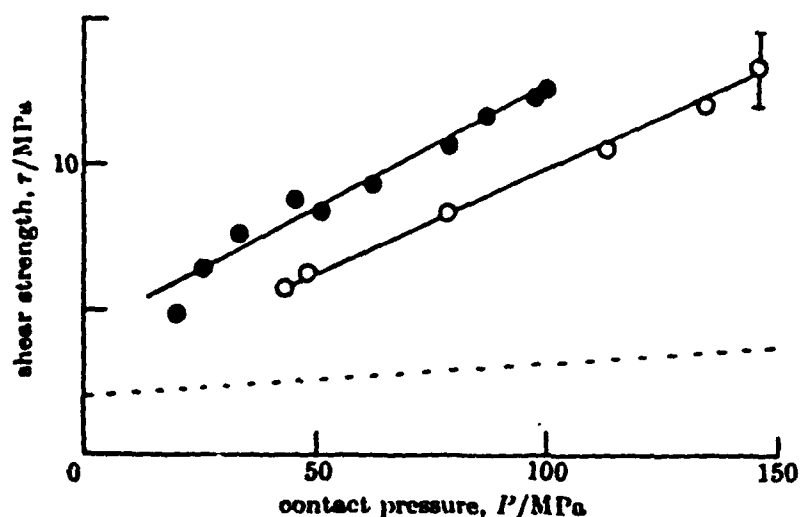
The shear strength of acid monolayers was also investigated by building up three layers of behenic acid (C_{22}) on each mica surface. The variation in τ with pressure was similar to that found for the monolayer. However a 20% reduction in the magnitude of τ was observed throughout the pressure range. The wear as monitored by the film thickness remained

unchanged during initiation of sliding and continuous motion. The accuracy of the thickness measurements was within a few angstroms so that major disruptions in the layers were readily detectable. They noted though that a chain tilt of 10° from the normal would not be distinguishable. The lack of any changes in the film thickness seemed to prove that shear only

Table 3: Constants in the Functional Relations between Shear strength and Pressure, Temperature, and Velocity. Measured by using Myristic, Stearic, and Behenic Acids. Briscoe and Evans.⁸

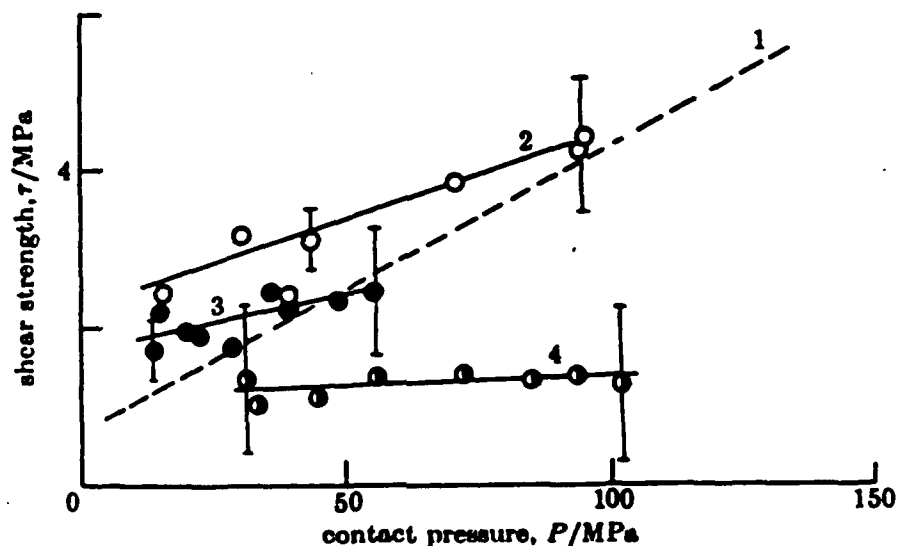
fatty acid ... value of n in ($C_{n-1}H_{2n-1}$) COOH	myristic 14	stearic 18	behenic 22	partially fluorinated stearic acid 10	calcium stearate 18
τ_0/MPa	0.6	0.6	2.2	3.4 ± 0.7	1.0
α	0.034	0.038	0.036	0.078 ± 0.07	0.003
$\tau\gamma'/\text{MPa}$	1.3	2.8	5.5	—	—
$\beta/(\text{MPa K}^{-1})$	0.019	0.042	0.048	—	—
τ_0^*/MPa	—	2.4	—	—	—
θ/MPa	—	0.42	—	—	—

Figure 7: Briscoe and Evans.⁸



The variation of shear strength with contact pressure for partially fluorinated stearic acid monolayers, $(C_7F_{15})(C_{10}H_{21})\text{COOH}$. The monolayers were deposited from 10^{-4} M calcium chloride at pH 4.4. The two sets of data were obtained from two separate experiments under similar conditions: $V = 3.6 \mu\text{m s}^{-1}$, $T = 21^\circ\text{C}$. Dashed line is for stearic acid under comparable conditions.

Figure 8: The Variation of Shear Strength with Contact Pressure for Stearic Acid Monolayers Deposited from 10^{-4} M Calcium Chloride at: 1-pH 4.7, 2-pH 5.9, 3-pH 7.7, 4-pH 9. $V = 3.6 \mu\text{m/s}$, $T = 21^\circ\text{C}$. Briscoe and Evans.⁸



occurs at the contact surface and not within the multilayers themselves and that the shear properties are virtually unchanged by the additional layers. This contradicts the commonly held view that shear strength decreases with film thickness. One difficulty with Briscoe's result for multilayers is that only one experiment with a limited number of layers was carried out or at least reported. Furthermore for their one experiment, a reduction in shear strength of 20% compared to a single layer was found. Their conclusion would be more valid if they had measured shear strength as a function of the number of layers.

The mechanism controlling shear in these experiments was attributed to a thermally activated process. With a mathematical model developed by Eyring for activated processes, and assuming that the motion of molecules in the monolayers is restricted by potential barriers equal to the Boltzmann factor times the effective vibration frequency of the moving unit, the equations for the dependence of shear strength on T , P , and V were derived. When the data was compared to the model, it was found that the data was not completely self-consistent with the model which was due to discrepancies in the shear strength-velocity behavior. I refer the reader to the reference for a more complete discussion of these results.

Briscoe and Evans concluded that the molecular parameters deduced from the Eyring model suggested that the rate-limiting step in the shear process involves the cooperative

motion of several molecules or parts of several molecules. The demarcation between blocks were regarded as dislocation lines in the interface plane. Therefore the interfacial shear involved the motion of dislocation lines.

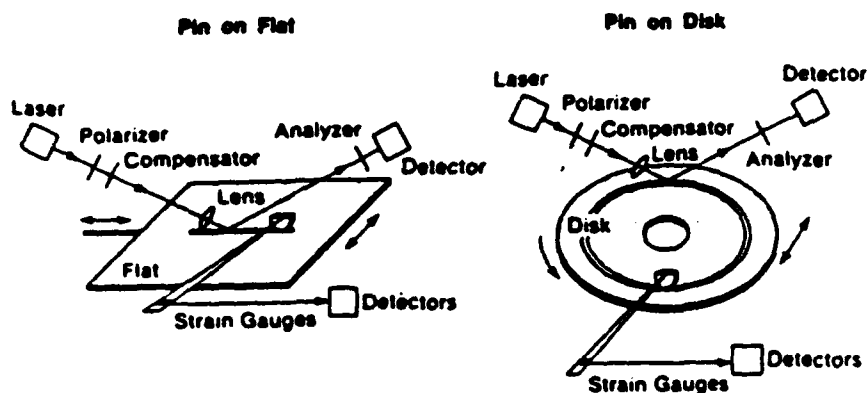
Because the model proposed by Briscoe and Evans did not fit the experimental data well, this suggests that there are other factors responsible for the friction behavior which were not taken into account. In bulk polymers, it is fairly well known that the friction behavior is dependent on both chemical structure and morphology.^{4,5} This is quite clear when comparing the wear behavior of HDPE, which is linear, highly symmetric, crystalline polymer, to that of LDPE which is branched and semicrystalline. The coefficient of friction for HDPE is low and delamination wear produces thin sheets of polymer films that are oriented parallel to direction of shear. LDPE on the other hand has a high coefficient of friction and delamination produces "lumpy" wear particles. In light of these results, it seems reasonable to assume that molecular packing of the monolayers would have a significant affect on their friction behavior. Molecular packing and orientation of condensed monolayers is highly influenced by the size of the atoms in the hydrocarbon chain and the substrate binding geometry of the ions used to make the salt forms of the LB materials. Rabe et. al.¹⁷ using near edge X-ray absorption have studied the chain orientation of arachidic acid monolayers with cadmium and calcium salt ions as well as cadmium salts of a semifluorinated fatty acid and tetradecylbenzoic acid on oxidized silicon. They found that cadmium arachidate chains are oriented almost perpendicular to the substrate surface while calcium arachidate chains are tilted 33° to the normal. Also the cadmium salts of the benzoate and fluorinated fatty acids were tilted considerably with respect to the surface normal. Measurements on arachidic acid alone showed that the monolayer had no net orientation of the bonds and was disordered. Another study by Swalen¹⁸ using arachidic acid puts the orientation of this monolayer at 30° to the substrate normal.

Similar to the study carried out by Briscoe and Evans, Novotny and Swalen¹⁹ studied the frictional behavior of cadmium arachidate mono- and multilayers adsorbed on oxidized silicon substrates. The goal was to determine whether a single layer or many layers provided better wear, how failure of these film occurred, and how transfer of film from one surface to another took place. Two types of devices were used to measure the friction behavior: a high speed pin-on-disk and a low speed pin-on-flat setup. Both devices used ceramic pin sliders. Wear of the monolayer and substrate was monitored in situ using scanning microellipsometry to measure the thicknesses of the wear tracks. Microellipsometry was also used to evaluate the transfer of monolayers to the sliders after each tribological run. These setups are shown in Figure 9 along with the experimental conditions.

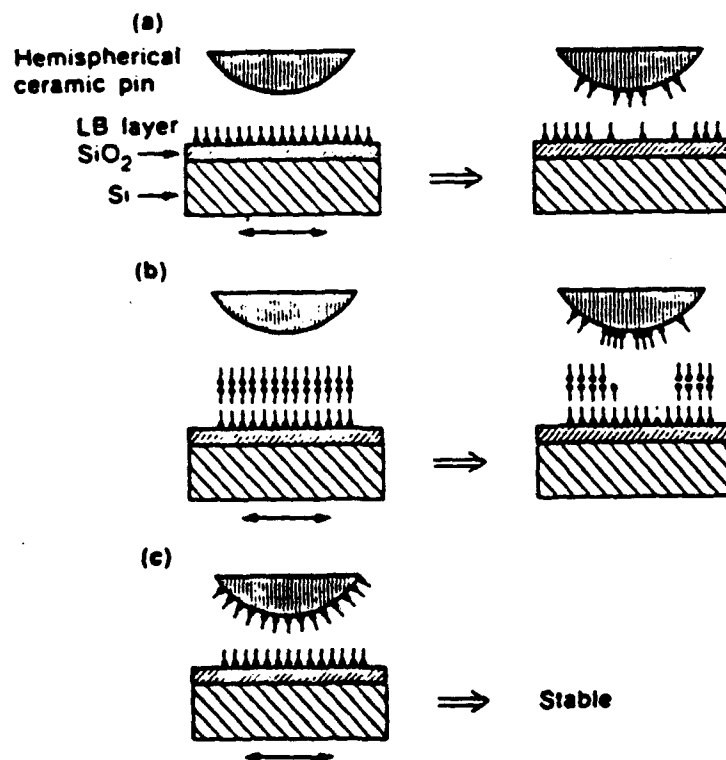
Their results indicated that a single monolayer of cadmium arachidate on either the silicon surface or slider did not significantly improve mechanical durability (wear occurred after several sliding cycles). However, when 3-13 multilayers were applied the friction coefficient decreased from 0.5 to 0.12 and the durability improved greatly. By microellipsometry, it was observed that all the layers, except the layer bound to the substrate, were removed after about one hundred sliding cycles. The monolayer next to the silicon surface retained its integrity for

thousands of sliding cycles with no significant deformation as measured by the thickness of the film. The best durability was found when both surfaces were covered with a single monolayer. The coefficient of friction again reached a value of 0.12 and no wear was observed after some million sliding cycles. The results with multilayers of cadmium arachidate at both

Figure 9: Novotny and Swalen.¹⁷



Low-speed pin-on-flat and pin-on-disk tribological setups with in situ scanning microellipsometry to profile wear of LB films.



Schematic representation of tribological experiments: (a) with flat or disk coated with an LB monolayer; (b) with flat or disk coated with multilayers; (c) with both surfaces coated with a monolayer.

surfaces paralleled the situation found for multilayers on a single surface i.e. the outer layers were removed after almost one hundred cycles leaving one monolayer next to the substrate. Even at the lowest contact pressures capable, damage to the outer LB layers occurred very rapidly.

The system which exhibited the best durability was clearly the system that had both surfaces covered by a monolayer of cadmium arachidate. Wear rates calculated as $W=A/N$ where A is the cross section of the wear track and N is the number of sliding cycles showed the multilayers to have $W = 0.2 \mu\text{m}^2/\text{cycle}$ and the monolayers $W = 2 \times 10^{-6} \mu\text{m}^2/\text{cycle}$. Novotny and Swalen rationalized their results as follows: the durability of their cadmium arachidate multilayers can be understood from its structure. Since the silicon surface is hydrophilic, the polar head group of the monolayer is bound to the surface with the hydrocarbon chain extending almost perpendicular to the substrate. Subsequent monolayers are also oriented perpendicular to the substrate with the tails of molecules in adjacent layers facing each other. The interactions between the head group and substrate are expected to be strong while the tails interaction is primarily weak Van der Waals forces. Therefore the critical contact pressure to break the layer-layer interactions is on the order of .02 MPa while that for the head group-substrate interaction is at least three times higher.

The results of Novotny and Swalen for multilayer instability are in direct contrast to those found by Briscoe and Evans where the durability of mono- and multilayers of behenic acid were comparable. There are several noticeable differences in the experimental procedures which should be investigated more thoroughly to try and account for this. Firstly, Briscoe and Evans used a behenic (C_{22}) fatty acid monolayer while Novotny and Swalen used a cadmium arachidate (C_{20}) soap. Claesson²⁰ doing stability measurements on monolayers of arachidic acid and cadmium arachidate with SFA found that the internal cohesion forces in cadmium arachidate multilayers were larger than that in the fatty acid analog. Given the fact that the contact pressures used by Briscoe were an order of magnitude higher than that used by Novotny, this along with Claesson's results makes the stability of the behenic acid multilayers seem remarkable!

However, there is one fact in favor of Briscoe's results. Claesson also pointed out that the weak link in multilayer LB structures is often the attractive forces between the polar head groups in adjacent layers, in the case of head-to-head or Y-type film deposition. In water or humid air these groups tend to be hydrated and the two opposing layers have a tendency to separate. In preparing their multilayer films, Briscoe made sure all the water was removed before testing by drying them in an oven at 35 C for 30 minutes. Novotny estimated that there was at least 1-2% trapped water in their films. This could account for the low shear strength of the outer layers of cadmium arachidate. This point could be moot if Novotny's results that a single monolayer at both wear surfaces is sufficient to prevent wear. Of course we would perhaps feel better if there were as many layers as possible between success and failure.

Briscoe's model of a thermally activated shear process also suggests that thermal stability is very important factor for monolayer lubricants. Thermal stability of LB films can be imparted by incorporation of metal ions which is routinely done when preparing fatty acid

soaps. These ions have good thermal conductivity as well as aid in anchoring the the monolayer to the substrate and increasing interlayer cohesion. Naselli et.al.²¹ have found that introducing aromaticity into the head also leads to increased thermal stability.

It has been shown that the presence of a remarkably thin layer of material, such as a Langmuir-Blodgett film, between two moving surfaces can substantially reduce friction and wear of the surfaces. These films are not only commercially important but are important as model systems for studying boundary lubrication. Friction studies with bulk polymer materials have indicated that molecular orientation, symmetry, and packing have direct effects on the friction coefficient and wear behavior of these materials. Future studies of boundary lubrication could use LB films to study these same effects and to elucidate the microscopic behavior of film molecules at the solid interface.

REFERENCES

1. Adamson, A., *Physical Chemistry of Surfaces*, fifth ed., Wiley Interscience, 1990.
2. Bowden, F., Tabor, D., *The Friction and Lubrication of Solids*, part I and II, Oxford University Press 1964.
3. Suh, N., *Tribophysics*, Prentice Hall Inc, 1986.
4. Tabor, D., *J. of Lubrication Tech*, **1981**, vol 103, 169.
5. Tewar, V., Sharma, S., Vasudevan, J., *Rev. Macromol. Chem. Phys.*, **1989**, c29(1), 1.
6. Lancaster, J., *Encyclopedia of Polym. Sci and Eng.*, second ed., Wiley Interscience, vol 1, 1, 1985.
7. Fort, T., *J. Phys. Chem.*, **1962**, 66, 1136.
8. Briscoe, B., Evans, D., *Proc. Roy. Soc. Lond.*, **1982**, A380, 389.
9. Homola, M., Israelachvili, J., McGuiggan, P., Lee, M., *Wear*, **1990**, 136, 65.
10. Erlandsson, R., Hadziannou, G., Mate, C., McClelland, G., Chiang, S., *J. of Chem. Phys.*, **1988**, vol 89, Iss 8, 5190.
11. Roberts, G., *Langmuir-Blodgett Films*, Plenum Press, 1990.
12. Gaines, G., *Insoluble Monolayers*, Interscience Pub., 1966.
13. Swalen, J., Allara, D., Andrade, J., Chadross, E., Garoff, S., Israelichvili, J., McCarthy, T., Murray, R., Pease, R., Rabolt, J., Wynna, K., Yu, H., *Langmuir*, **1987**, 3, 932.
14. Kowel, S., Selfridge, R., Eldering, C., Matloff, N., Stroeve, P., Higgins, B., Sprintvasm, M., Coleman, C., *Thin Solid Films*, **1987**, 152, 377.
15. Seto, T., Nagai, T., Ishimoto, C., Watanabe, H., *Thin Solid Films*, **1985**, 134, 101.
16. Suzuki, M., Saotome, Y., Yanacisawa, M., *Thin Solid Films*, **1988**, 160, 457.
17. Rabe, J., Swalen, J., Outka, D., Stohr, J., *Thin Solid Films*, **1988**, 159, 275.
18. Swalen, J., *Thin Solid Films*, **1987**, 152, 154.
19. Novotny, V., Swalen, J., *Langmuir*, **1989**, 5, 485.
20. Claesson, P., Berg, J., *Thin Solid Films*, **1989**, 176, 157.
21. Naselli, C., Rabe, J., Rabolt, J., Swalen, J., *Thin Solid Films*, **1985**, 134, 173.